JULY 01 2004

A theoretical study for the propagation of rolling noise over a porous road pavement

Wai Keung Lui; Kai Ming Li

J. Acoust. Soc. Am. 116, 313–322 (2004)
https://doi.org/10.1121/1.1751153

A theoretical study for the propagation of rolling noise over a porous road pavement

Wai Keung Lui and Kai Ming Li[a)]
Department of Mechanical Engineering, The Hong Kong Polytechnic University, Hung Hom, Hong Kong

(Received 10 April 2003; revised 18 February 2004; accepted 29 March 2004)

A simplified model based on the study of sound diffracted by a sphere is proposed for investigating the propagation of noise in a hornlike geometry between porous road surfaces and rolling tires. The simplified model is verified by comparing its predictions with the published numerical and experimental results of studies on the horn amplification of sound over a road pavement. In a parametric study, a point monopole source is assumed to be localized on the surface of a tire. In the frequency range of interest, a porous road pavement can effectively reduce the level of amplified sound due to the horn effect. It has been shown that an increase in the thickness and porosity of a porous layer, or the use of a double layer of porous road pavement, attenuates the horn amplification of sound. However, a decrease in the flow resistivity of a porous road pavement does little to reduce the horn amplification of sound. It has also been demonstrated that the horn effect over a porous road pavement is less dependent on the angular position of the source on the surface of tires. [DOI: 10.1121/1.1751153]

PACS numbers: 43.50.Lj [DKW] Pages: 313–322

I. INTRODUCTION

The mechanisms of the generation of rolling noise caused by the interaction between a tire and the surface of a road[1–4] have received considerable attention over the past few decades. The noise comes from the vibrations of tires, the deflections from the surface of the tires, and the resulting displacement of air in the gap between the tire and the road.[4] In this case, the propagation of noise is thus confined to a small area enveloped by the surface of the road and the tire belt, forming a hornlike geometry. This hornlike configuration leads to a substantial amplification of the sound that is radiated. Schaaf and Ronneberger[5] demonstrated this effect experimentally, and theoretically identified this so-called ''horn effect'' by a simple image source model. The phenomenon of the horn effect amplification was also confirmed experimentally by Iwao *et al.*[1]

Kropp *et al.*[6] suggested a theoretical model based on multipole synthesis.[7] The model can provide a reasonable prediction of noise levels at mid and high frequencies for a tire placed on a hard surface. However, it overestimates the horn amplification effect at low frequencies. Since the Kropp model is a two-dimensional one, the model can only be valid for estimating the amplification of sound when the receiver is located in the plane of a tire. Although a three-dimensional (3D) model of a tire can, by virtue of the boundary element method (BEM),[8,9] be used for this purpose, the BEM can be a time-consuming tool for predicting the horn effect for practical geometries. Moreover, the BEM cannot be used in a parametric study of the influence of porous ground on the horn amplification. In the meanwhile, researchers have endeavored to develop three-dimensional (3D) analytical models based on the modal decomposition of the sound pressure[10] and on the asymptotic theories[11] for modeling the horn effect. However, these models either do not consider the effect of impedance ground or are somewhat inadequate in light of the recent advances in predicting the propagation of sound outdoors.[12–14] It is also worth pointing out that the two asymptotic models presented by Kuo *et al.*,[11] a ray theory for high frequencies and a compact body scattering model for low frequencies, were found to be accurate on a typical tire at frequencies of above 3 kHz and below 300 Hz, respectively. However, at the frequencies of practical interest (approximately 500–2500 Hz), it is not possible for the asymptotic models to provide satisfactory predictions.

In view of the intrinsic limitations of the existing numerical methods and analytical models for predicting the horn amplification, and the increase in interest in using porous pavement,[15–17] especially double-layer porous pavement,[18,19] to reduce tire/road noise, it is thus desirable to offer a simplified theoretical model to allow highway designers to carry out a parametric study when selecting appropriate materials for porous road pavement. The purpose of this paper is to explore a simplified theoretical model to account for the amplification of noise due to the propagation of sound in the tire/road gap over a porous road pavement. The theoretical model is centered on a recent analytical formulation to study the sound diffracted by a sphere above an impedance ground.[20,21] In Sec. II, we explain and justify the choice of our analytical model, as there are many other numerical models[6,8,11] devoted to the study of the acoustic interaction between tires and road. Section III gives numerical predictions based on our analytical formulation. These numerical results are compared with the published experimental data and theoretical predictions based on other computationally intensive schemes. A parametric study of the influence of porous ground on the horn effect is discussed in Sec. IV. Finally, in Sec. V, we offer some concluding remarks.

[a)]Author to whom correspondence should be addressed; Electronic mail: mmkmli@polyu.edu.hk

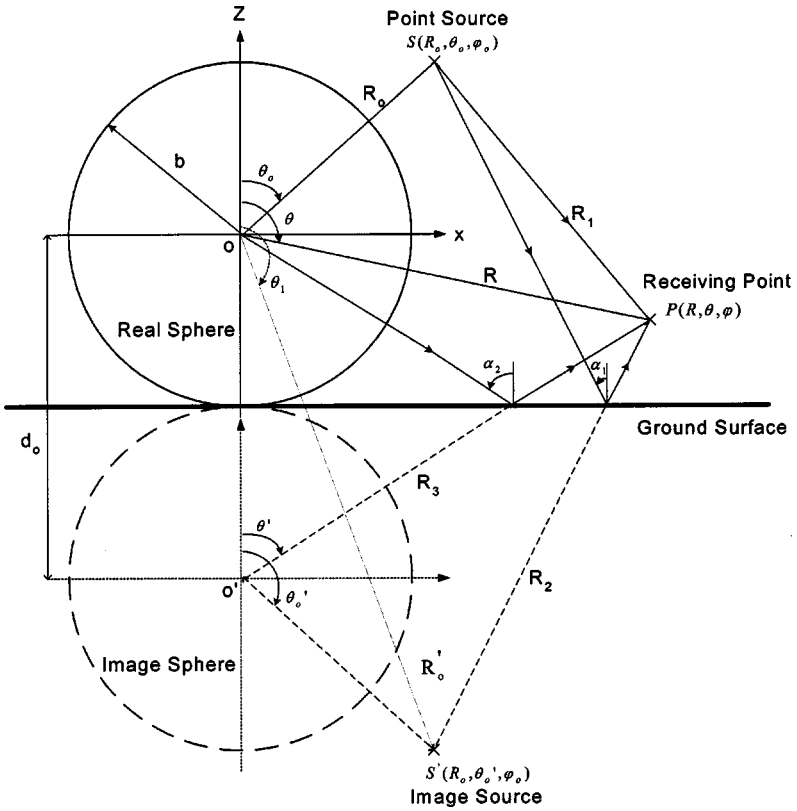

FIG. 1. Geometrical configuration of a sphere on flat ground irradiated by a point source.

II. THEORETICAL FORMULATION

A. Justifications for the use of a simple theoretical model

The dependence of the horn effect on different geometrical parameters such as the radius of the curvature of the tire shoulders, the load, the width of the tire, and the geometrical configurations of the source/receiver have been investigated through experiments, the formulation of exact boundary element (BEM)[8] and other asymptotic theories.[11] The experimental measurements showed that the effect of the horn amplification accounted for about 10–20 dB, with the maximum amplification occurring at the plane of the tire. In view of the fact that the amplification of sound reaches a maximum at the plane of the tire, as shown by the published experimental results,[6,8,11] we hypothesize that the horn effect induced by the semi-closed space formed between the curved surface of a sphere and the ground surface is similar to that created by the hornlike geometry formed between the tire belt and the surface of the road. Although this hypothesis may at first appear questionable, we will validate it through detailed comparisons of the numerical predictions using the published experimental data described in Sec. III.

B. Review of sound diffracted by a sphere above an extended reaction ground

When an object is subject to radiation from a point source located at $\mathbf{x}_s$, the total sound field at point $\mathbf{x}$ is governed by the Helmholtz equation, expressed in terms of a scalar velocity potential, ϕ, as follows:

$$\nabla^2\phi + k_o^2\phi = -\delta(\mathbf{x}-\mathbf{x}_s), \tag{1}$$

where $k_o = \omega/c$ is the wave number, ω is the angular frequency of the source, and c is the sound speed in air. For a sphere resting on a ground surface, the total sound field at the receiver is contributed by the direct waves, by scattered waves from the sphere, and by waves disseminating from the image source and the image sphere, as shown in Fig. 1. The origin is taken as the center of the sphere. In this situation, the acoustical properties of the porous medium are crucial in determining the sound field produced due to the combination of direct and boundary-reflected sound waves. In our earlier study,[20,21] we developed a numerical scheme to compute the diffraction of sound by a sphere located above an impedance ground. The scheme was based on the expansion of the wave field in terms of a series of associated Legendre functions. Here, we extend the solution to model the corresponding sound field above an extended reaction ground. In particular, the road pavement is modeled as either a single or double porous layer above a hard-backed layer. In fact, Bérengier *et al.*[16] used a hard-back layer model to study the acoustical characteristics and propagation effects of porous road pavements.

The effect of a single or double porous layer above a hard-backed layer on the radiation from a point source can be modeled by an approximate analytical solution developed by Li *et al.*[14] for the reflection of a spherical wave. By introducing an effective admittance, β_g, the sound field contributed from the point source above a hard-backed layer surface can be approximated by

$$\phi_T^i = \frac{e^{ik_o R_1}}{4\pi R_1} + Q_1 \frac{e^{ik_o R_2}}{4\pi R_2}, \tag{2}$$

where

$$Q_1 = V + (1-V)F(\varpi), \tag{3a}$$

$$V = \frac{\cos\alpha_1 - \beta_g}{\cos\alpha_1 + \beta_g}, \tag{3b}$$

$$F(\varpi) = 1 + i\sqrt{\pi}\varpi e^{-\varpi^2}\,\mathrm{erfc}(-i\varpi), \tag{3c}$$

$$\varpi = +\sqrt{\frac{1}{2}ik_o R_2}(\cos\alpha_1 + \beta_g). \tag{3d}$$

For a single porous layer above a hard-backed layer, the effective admittance is

$$\beta_g = -im_1\sqrt{n_1^2 - \sin^2\alpha_1}\,\tan(k_o l_1\sqrt{n_1^2 - \sin^2\alpha_1}), \tag{4}$$

and for a double layer with a hard backing, the effective admittance can be determined according to

$$\beta_g = -im_1\sqrt{n_1^2 - \sin^2\alpha_1}\left\{\frac{\tan(k_o l_1\sqrt{n_1^2 - \sin^2\alpha_1}) + \overline{g_1}\tan(k_o l_2\sqrt{n_2^2 - \sin^2\alpha_1})}{1 - \overline{g_1}\tan(k_o l_1\sqrt{n_1^2 - \sin^2\alpha_1})\tan(k_o l_2\sqrt{n_2^2 - \sin^2\alpha_1})}\right\}, \tag{5}$$

where

$$\overline{g_1} = \frac{m_2\sqrt{n_2^2 - \sin^2\alpha_1}}{m_1\sqrt{n_1^2 - \sin^2\alpha_1}}, \tag{6a}$$

$$n_j = k_j/k_o \quad \text{and} \quad m_j = \rho_o/\rho_j \quad \text{with} \quad j = 1,2. \tag{6b}$$

Here, ρ_o is the density of air, g_1 is a dimensionless ratio characterizing the change of media properties from the first layer to the second, R_2 is the distance between the image source and the field point, α_1 is the angle of incidence of the reflected wave, and l_1 and l_2 are the thickness of the first and second layers, respectively. According to the phenomenological model for porous pavement proposed by Bérengier *et al.*,[16] the complex wave number and characteristic impedance can be written as

$$k = k_o q F_\mu^{1/2}[\gamma - (\gamma-1)/F_\theta]^{1/2}, \tag{7}$$

$$Z_c = (\rho_o c q/\Omega)F_\mu^{1/2}[\gamma - (\gamma-1)/F_\theta]^{-1/2}. \tag{8}$$

The functions

$$F_\mu = 1 + if_\mu/f \tag{9}$$

and

$$F_\theta = 1 + if_\theta/f \tag{10}$$

are related to the viscous and thermal dependencies, which are given respectively by

$$f_\mu = \Omega R_s/(2\pi\rho_o q^2), \tag{11}$$

$$f_\theta = R_s/(2\pi\rho_o N_{\mathrm{pr}}). \tag{12}$$

In the above equations, γ is the specific heat ratio, N_{pr} is the Prandtl number, R_s is the airflow resistivity of the porous structure, Ω is the porosity of the air-filled connected pores, and q^2 is the tortuosity. These last three parameters can be independently determined, directly or indirectly, which makes this simple model for porous road pavements attractive. In addition, the density ratio m_1, the index of refraction n_1, and the normalized surface impedance $Z = Z_c/\rho_o c$ are related according to the following relationship:

$$\frac{1}{Z} = m_1 n_1. \tag{13}$$

Hence, by using Eqs. (4)–(13), we can determine the effective admittance for a given frequency and other physical parameters.

Since the scattered waves from the sphere above a ground surface are spherically spreading waves, the total scattering sound field due to the presence of a hard-backed porous ground can be calculated by[20,21]

$$\phi_T^s = \phi^s + Q_2\phi_r^s, \tag{14}$$

where ϕ^s is the scattered sound field from a real sphere in free space and ϕ_r^s is the scattered sound field from the image sphere. The spherical wave reflection coefficient Q_2 for a scattered wave reflection on an impedance ground can be obtained in a similar formulation as Eq. (3a). In fact, Q_2 can be computed by replacing α_1 and R_2 in Eqs. (3)–(6) with α_2 and R_3, respectively, where R_3 is the distance of separation between the center of the image sphere and the field point, and α_2 is the angle of incidence of the scattered wave on the porous layer. The total sound field above a hard-backed porous layer can now be represented in a real spherical coordinates system, which consists of four components: direct source, scattered waves from the real sphere, image source, and scattered waves from the image sphere, as follows:[20,21]

$$\phi^T=\phi^i+Q_1\phi_r^i+\phi^s+Q_2\phi_r^s$$

$$=\sum_{n=0}^{\infty}\sum_{m=0}^{n}a_{mn}h_n^{(1)}(k_oR_o)j_n(k_oR)P_n^m(\cos\theta)P_n^m(\cos\theta_o)\cos m(\varphi-\varphi_o)+Q_1\sum_{n=0}^{\infty}\sum_{m=0}^{n}a_{mn}h_n^{(1)}(k_oR_0')j_n(k_oR)$$

$$\times P_n^m(\cos\theta)P_n^m(\cos\theta_1)\cos m(\varphi-\varphi_o)+\sum_{n=0}^{\infty}\sum_{m=0}^{n}b_{mn}h_n^{(1)}(k_oR_o)h_n^{(1)}(k_oR)P_n^m(\cos\theta)P_n^m(\cos\theta_o)\cos m(\varphi-\varphi_o)$$

$$+Q_2\sum_{q=0}^{\infty}\sum_{m=0}^{q}(-1)^{m+q}b_{mq}h_q^{(1)}(k_oR_o)P_q^m(\cos\theta_o)\sum_{n=m}^{\infty}A_{mn}^{mq}(k_od_o)j_n(k_oR)P_n^m(\cos\theta)\cos m(\varphi-\varphi_o), \quad (15)$$

where

$$a_{mn}=\frac{i(n-m)!(2n+1)(2-\delta_{m0})k_o}{4\pi(n+m)!}, \quad (16)$$

and δ_{m0} is a Kronecker delta function that vanishes if $m\neq 0$. The translation coefficient $A_{mn}^{mq}(k_od_o)$ is given in Refs. 20 and 21. The unknown scattering coefficient b_{mn} can be determined by imposing the rigid boundary condition on the surface of the sphere if it is regarded as acoustically hard. As a result, we can get a set of coupled linear complex equations for solving b_{mn} in a matrix form, as follows:

$$\mathbf{XB}=\mathbf{D}. \quad (17)$$

The diagonal elements of **X** are

$$X_{mn}=h_n^{(1)}(k_oR_o)P_n^m(\cos\theta_o)+Q_2T_n(-1)^{m+n}h_n^{(1)}$$
$$\times(k_oR_o)P_n^m(\cos\theta_o)A_{mn}^{mn}(k_od_o), \quad (18a)$$

the off-diagonal elements of **X** are

$$X_{nq}=Q_2T_n(-1)^{m+q}h_q^{(1)}(k_oR_o)P_q^m(\cos\theta_o)A_{mn}^{mq}(k_od_o), \quad (18b)$$

and the elements of the vector **D** are

$$D_n=-a_{mn}T_n[h_n^{(1)}(k_oR_o)P_n^m(\cos\theta_o)+Q_1h_n^{(1)}(k_oR_o')$$
$$\times P_n^m(\cos\theta_1)], \quad (18c)$$

with

$$T_n=\frac{j_n'(k_ob)}{h_n'(k_ob)}. \quad (18d)$$

The system of complex equations in Eq. (17) can be truncated to an order of N; that is, the number of sums from n or $q=0$ to N, depending on the degree of accuracy required. The complex matrix **X** has an order of $(N+1-m)\times(N+1-m)$, and the complex vectors **B** and **D** have dimensions of $(N+1-m)$ for each m, where m ranges from 0 to N. The details of the numerical techniques, which can be found elsewhere,[20,21] are not repeated in this paper for brevity.

III. COMPARISONS WITH PUBLISHED RESULTS

According to the hypothesis stated in Sec. II above, the tire belt can be replaced by a sphere for predicting the horn effect of a tire/road interaction. In order to apply this simplified model to investigate the influence of porous ground, it is important to validate the hypothesis. There are published experimental results and BEM calculations for the interaction of a tire with hard ground. In this section, these published results are compared with the predictions computed by the simplified model.

Based on the experimental configuration described in Ref. 8, the following geometrical configuration is used (unless stated otherwise) for all of the numerical calculations throughout this section. The sphere, which has a diameter of 0.64 m, is placed on the ground, and a point source is located 2.57 m from the center of the sphere and 0.72 m above the surface of the ground. In the graphs, the amplification due to the horn effect is plotted against the frequency. Throughout this section, amplification is defined as the difference in sound levels with and without the presence of the sphere. Equation (15) is used in the computations, with Q_1 and Q_2 set to 1 in the case of hard ground. For all of the simulations in this section, the receiver is located on the ground at a distance d from the contact point and at an offset distance o from the center of the sphere (see Fig. 2). The computed results are plotted for comparison with the published experimental results.

Figure 3, which is extracted from Fig. 11 of Ref. 8, shows the experimental measurements for a cylinder and an unloaded tire for different distances d from the contact point. In the same figure, we also show the theoretical predictions for the amplification of sound, calculated by assuming a hard sphere rested on a hard ground for the same geometrical configurations. In these measurements and numerical predic-

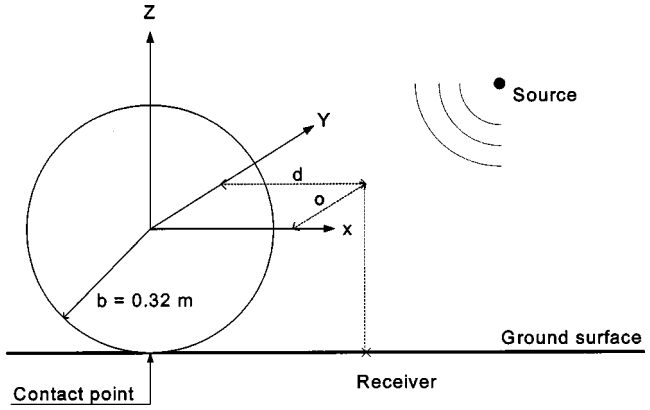

FIG. 2. A rigid sphere on flat ground to simulate the horn effect. The receiver is located on the ground at a distance d from the contact point (the center of the sphere) and at an offset distance o from the contact point.

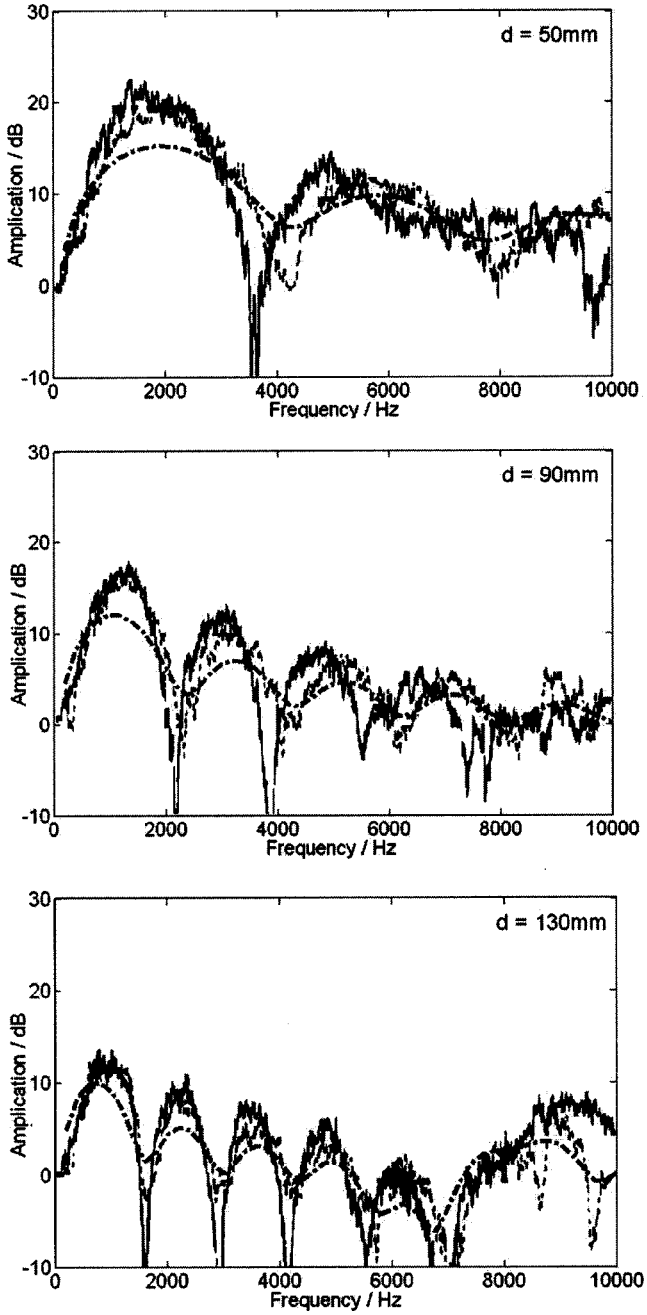

FIG. 3. Comparison of sound amplification by a rigid sphere simulation model to the experimental measurements of cylinder/tire (Fig. 11 in Ref. 8) on a hard ground for different distances *d*. The receiver is located at the centerline of the scatter. The solid line and dotted line represent the experimental results of a cylinder and tire, respectively. The dash-dotted line represents the result predicted by the simulation model.

tions, the receiver was located at the centerline, $o=0$, of the respective scatter. It can be seen from Fig. 3 that, according to our model, the predicted dips are shallower than those shown in the experimental measurements for the cylinder and the tire. According to Graf *et al.* with respect to the BEM results shown in Fig. 12 of Ref. 8, the effect of the rounded shoulders of the tire can broaden the dips of the acoustic interferences, reduce the maximum amplification, and shift the dips to higher frequencies. This can be confirmed in our numerical predictions because a sphere has a much larger radius curvature of the round edges than an unloaded tire.

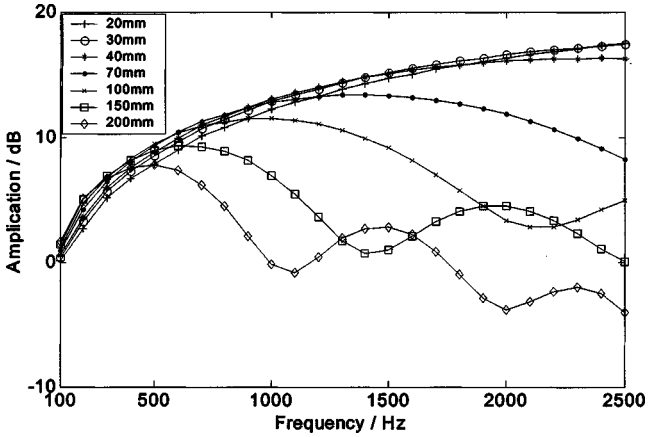

FIG. 4. Dependence of sound amplification on *d* by a rigid sphere simulation model (compared to Fig. 4 in Ref. 8).

Not surprisingly, the predicted amplification spectra are in closer agreement with the measured results of an unloaded tire than with the corresponding results of a cylinder. This is understandable, because the hypothesis of using a sphere to replace a tire belt is used in our numerical simulations.

The dependence of the amplification on *d* is plotted in Fig. 4. It is obvious that at low frequencies the amplification is independent of *d*. The amplifications give almost no differences for sufficiently small values of *d* (less than 40 mm). Our theoretical predictions show good qualitative agreement with the trends shown in the experimental observations found in Ref. 8; see their Fig. 4. In Fig. 5 of this paper, the results of the simulation of different *d* at various offset distances *o* of the receiver away from the center of the sphere are shown for comparison with the experimental measurements obtained from Fig. 16 in Ref. 8. Our theoretical model is consistent with this in predicting the general trend of the amplification due to the horn effect: it decreases as the offset distance increases. We note that, as shown in Figs. 4 and 5, the interference minima are less distinct in the predicted results according to the numerical model presented in this paper. This is due to the corner effect of the sphere.

The ability of the proposed simulation model to describe the amplification of sound by a smooth tire is compared with the ray theory developed by Kuo *et al.*,[11] as shown in Fig. 6. The numerical results predicted by the ray theory and the measurements given in Fig. 6 are extracted from Fig. 5 of Ref. 11. The locations of the microphone and receiver are given in Fig. 6, where *d* is the distance of the source from the contact patch, *L* is the distance of the receiver from the contact patch, and ø is the angle made by the receiver with the ground (see Figs. 2 and 5 of Ref. 11). It is of interest to point out that our proposed simulation model seems to give closer agreement with the experimental data than the ray model. However, as in our previous observations, the interference dips predicted by our simulation model are consistently shallower than those obtained by the ray model and measurements.

It is worth noting that use of a sphere to represent a tire has somewhat limited the quantitative accuracy of the numerical model proposed in Sec. II. Indeed, it can be seen from Fig. 3 that the BEM results of a cylinder and the ex-

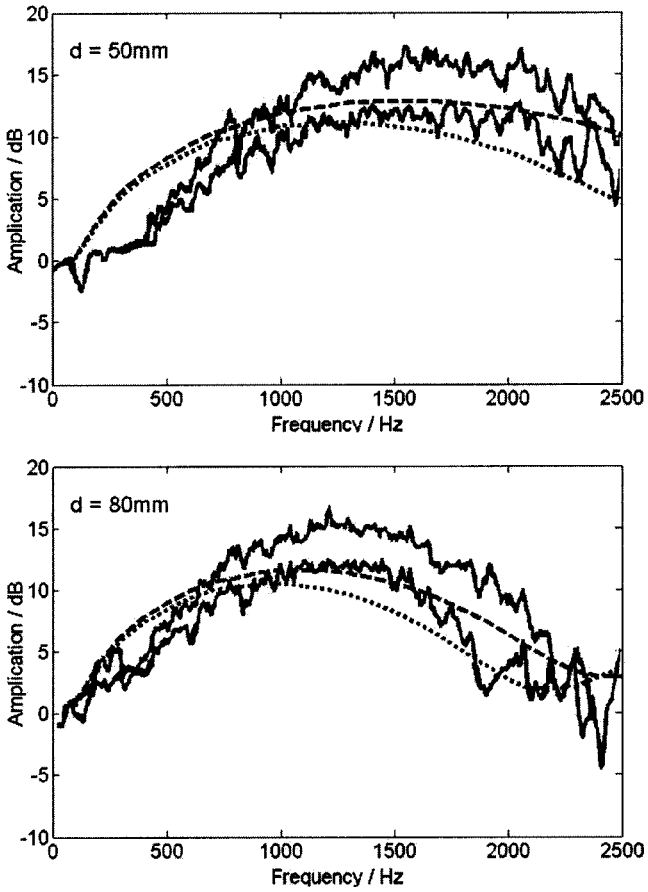

FIG. 5. Comparison of sound amplification by a rigid sphere simulation model to the experiments for a cylinder (Fig. 16 in Ref. 8) on a hard ground for different offset distances o from the centerline of the scatter. The solid lines represent the experimental results of a cylinder. The dashed line and dotted line represent the simulation results of an offset distance 5 and 8 cm, respectively.

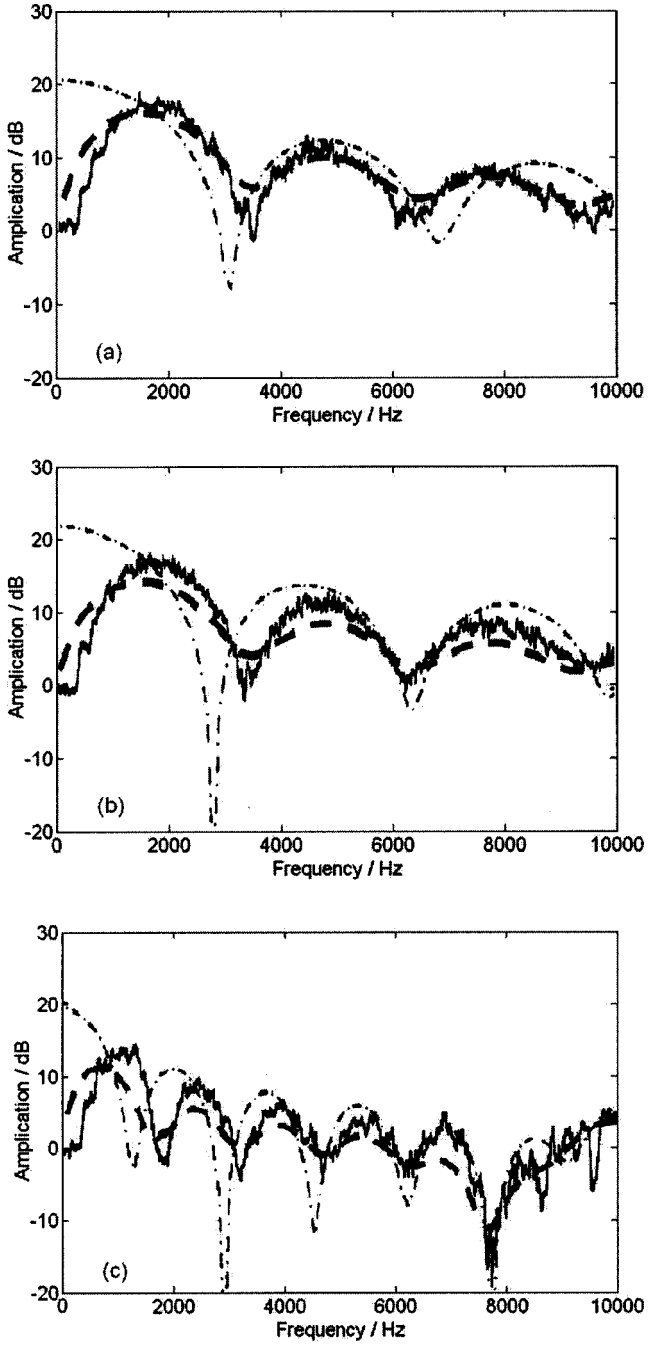

FIG. 6. Comparison of sound amplification by a rigid sphere simulation model with smooth tire measurement and ray theory given in Fig. 5 of Ref. 11. The solid line and dash-dotted line represent results from smooth tire measurement and ray theory, respectively. The dashed line represents the simulation result. (a) $d=60$ mm, $(L,\phi)=(2.67\text{ m},15°)$; (b) $d=60$ mm, $(L,\phi)=(1.92\text{ m},2.4°)$; (c) $d=120$ mm, $(L,\phi)=(2.67\text{ m},15°)$.

perimental data of a tire are different from our predicted results by an order of 5 dB. However, we stress that an objective of our present study is to exploit the acoustic characteristic of porous road pavement for reducing the amplification of sound due to the horn effect. As our model has proved to be accurate in predicting the general trend of the amplification spectra at a much reduced computational time especially at high frequencies, we shall use it in a parametric study of porous road pavement, as detailed in Sec. IV. This detailed study can lay a foundation to optimize the design of porous road pavements for reducing noise caused by the interaction between tire and road.

Next, we verify the validity of Li's approximate analytical model[14] for the propagation of sound above a hard-backed layer of porous ground, as follows. Bérengier's published results (Fig. 7 of Ref. 16) are compared with the numerical predictions according to the approximate model for porous ground (see Fig. 7). The geometrical configurations and other details of the porous pavement can be found in Ref. 16. We can confirm that Li's prediction results are consistent with Bérengier's numerical results. Hence, our proposed sound propagation model for a spherical wave propagated above a porous road pavement can be confidently adopted to study the horn effect above a porous road pavement.

Finally, we end this section by comparing our predictions with those calculated by a 2D-BEM model for a rigid cylinder on porous ground. The predicted results of the 2D-BEM model are taken from Fig. 2 of Ref. 10. Figure 8 shows the geometrical locations of a point source and receiver of the simulation. In this numerical example and other simulations shown in Sec. IV, unless otherwise stated, the sound source is assumed to be localized at a single point on the

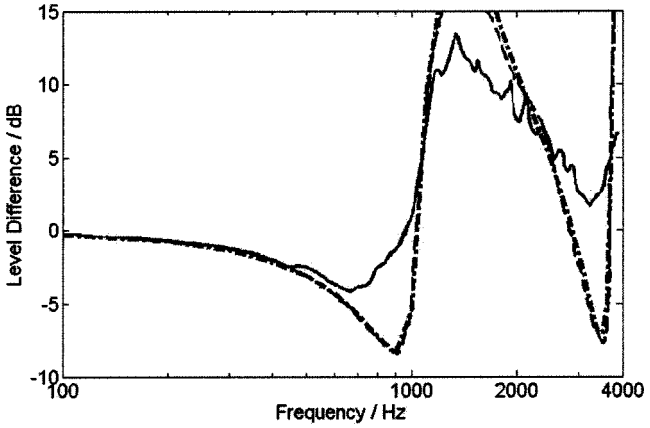

FIG. 7. Reproduction of Bérengier's results (Fig. 7 in Ref. 16) of level differences obtained above a porous asphalt using Li's approximate analytical model for sound propagation above a finite hard-backed layer of porous ground.[14] Solid line: measurement results by Bérengier; dashed line: results predicted by Bérengier; dash-dotted line: results predicted by Li.[14]

surface of a sphere with a radius of 0.3 m and situated at an angle of $\psi = 5°$ measured from the vertical axis. The receiver is located at a horizontal distance of 1 m from the contact point of the sphere and situated at a height of 0.3 m above the porous pavement. The acoustical structural parameters of the porous layer are $R_s = 20\ \mathrm{kN\,s\,m^{-4}}$, $\Omega = 15\%$, $q^2 = 3.5$, and $l_1 = 0.04$ m. It is shown in Fig. 9 that our model gives comparable spectra as that computed by the 2D-BEM model. Again, the difference in the amplification factor is of an order of about 5 dB. This observation is consistent with the earlier simulation results for hard ground, shown in Fig. 3. It is worth pointing out that the discrepancies between the predictions made by our model and the 2D-BEM model for porous ground are less than that for hard ground. The differences in magnitude are less than 3 dB in the frequency range between 800 Hz to 4000 Hz in the case of the amplification of sound over porous ground.

IV. A PARAMETRIC STUDY OF POROUS ROAD PAVEMENT ON THE HORN EFFECT

Section III presents a set of comprehensive numerical comparisons with published experimental data and theoretical predictions of horn amplification above the surface of the ground. It is reassuring to find that the numerical results of our simulation model can give a reasonable agreement with the general trend of the published experimental data and the-

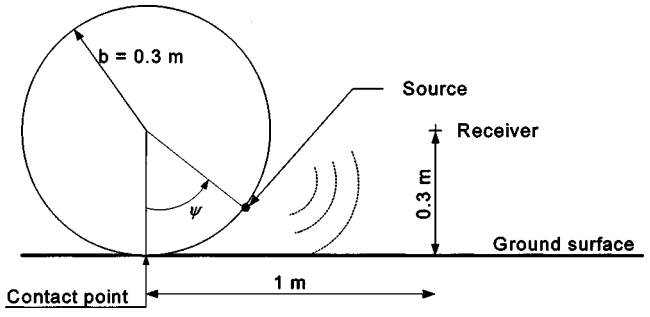

FIG. 8. Localized sound source located on the surface of the sphere at an angle ψ measured from the vertical axis.

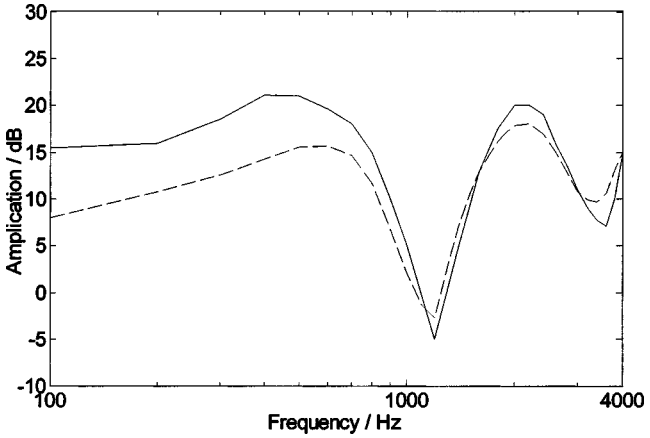

FIG. 9. Comparison of the amplification of sound by a rigid sphere simulation model to a 2D-BEM model for a rigid cylinder on porous ground. The acoustical structural parameters of the porous layer are $R_s = 20\,000\ \mathrm{N\,s\,m^{-4}}$, $\Omega = 15\%$, $q^2 = 3.5$, and $l_1 = 0.04$ m. (Solid line: 2D-BEM model; dotted line: rigid sphere simulation model.)

oretical predictions based on other numerical schemes. We can now use our prediction model to explore the effect of sound propagation due to a point source located in the gaps between the tire and a porous road pavement. The road pavement has either a single layer or double layers. The influence of porous road pavement on the horn effect can be investigated by using Eq. (15). The phenomenological model as described in Eqs. (7)–(12) can be employed to determine the effective admittance of the porous layer by using Eq. (13). The horn effect considered in this section is the difference in sound pressure level due to a localized sound source on the surface of the tire with and without porous ground. The source/receiver configurations of the following examples are given in Fig. 8.

In Fig. 10, we show the influence of the thickness of a porous layer on the reduction in the horn amplification of sound radiating from tires. In these simulations, the acoustical structural parameters of the porous layer are $R_s = 20\ \mathrm{kN\,s\,m^{-4}}$, $\Omega = 15\%$, $q^2 = 3.5$, with the thickness of the porous layer varying from 0.0 m (hard ground) to 0.04 m at

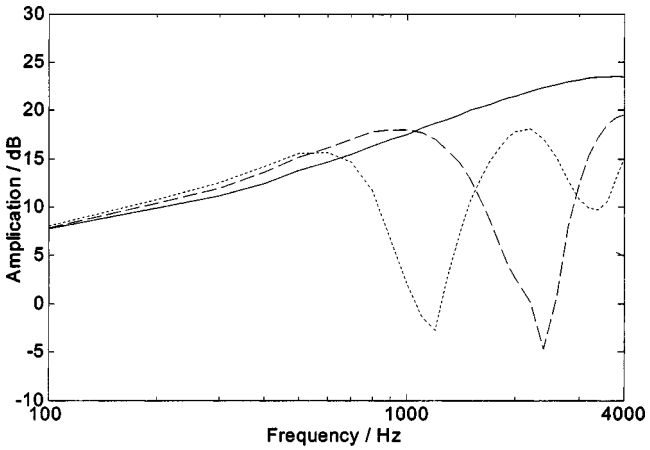

FIG. 10. Influence of the thickness of a porous road pavement on the horn effect. The acoustical structural parameters of the porous layer: $R_s = 20\,000\ \mathrm{N\,s\,m^{-4}}$, $\Omega = 5\%$, and $q^2 = 3.5$. (Solid line: hard ground; dashed line: $l_1 = 0.02$ m; dotted line: $l_1 = 0.04$ m.)

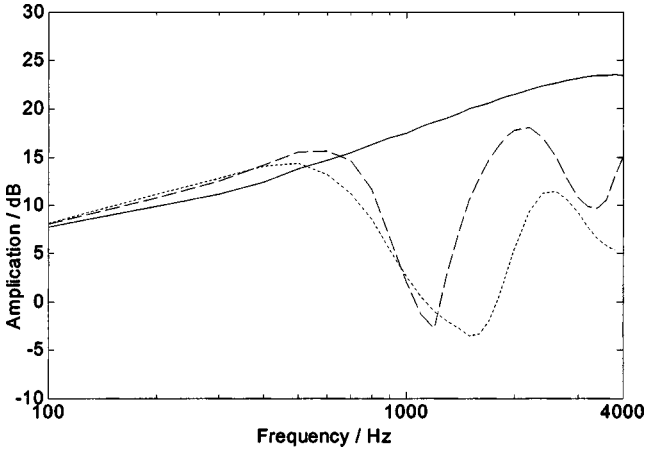

FIG. 11. Influence of the porosity of a porous road pavement on the horn effect. The acoustical structural parameters of the porous layer: $R_s = 20\,000\ \mathrm{N\,s\,m^{-4}}$, $q^2 = 3.5$, and $l_1 = 0.04$ m. (Solid line: hard ground; dashed line: $\Omega = 15\%$; dotted line: $\Omega = 30\%$.)

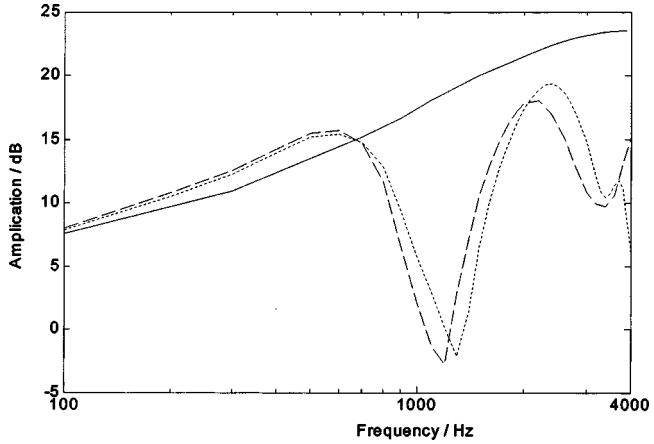

FIG. 12. Influence of the flow resistivity of a porous road pavement on the horn effect. The acoustical structural parameters of the porous layer: $\Omega = 15\%$, $q^2 = 3.5$, and $l_1 = 0.04$ m. (Solid line: hard ground; dashed line: $R_s = 20\,000\ \mathrm{N\,s\,m^{-4}}$; dotted line: $R_s = 5000\ \mathrm{N\,s\,m^{-4}}$.)

a step of 0.02 m. A porous road pavement can effectively suppress the amplification of sound due to the horn effect by creating interference minima in the amplification spectrum. The interference ''dips'' shift to higher frequencies when the thickness of the porous layer is reduced. Obviously, the overall effectiveness of the porous road pavement in reducing noise will decrease as the thickness of the layer decreases. For instance, there is only one interference dip in the dominant frequency range of the noise of a rolling tire, i.e., 500 to 4000 Hz, at a layer thickness of 0.02 m.

Figure 11 presents another important piece of information for investigating the material properties of a porous layer on the horn effect. It shows the effect of the porosity of a porous layer on the horn amplification of sound. In this example, the acoustical structural parameters of the porous layer are chosen to be $R_s = 20\ \mathrm{kN\,s\,m^{-4}}$, $q^2 = 3.5$, and $l_1 = 0.04$ m. The respective porosity with $\Omega = 0\%$ (for a hard ground), 15%, and 25% are shown in the same figure for ease of comparison. As expected, a higher porosity can provide a better attenuation of the horn effect by reducing the magnitude of the sound amplification. The finding is consistent with the conclusion drawn in Ref. 15. With regard to the flow resistivity of a porous layer, the change in its value does not do much to alter the sound spectrum, as evidenced in Fig. 12. Nevertheless, some noticeable changes can still be observed at frequencies higher than 3500 Hz.

Recent studies[17–19] have identified that a double layer of porous road pavement can better reduce the road traffic noise. Its application in road construction has received attention in recent years. Hence, the influence of a double layer of porous road pavement on the horn amplification of sound is worth exploring in the present study. For practical significance and numerical convenience, two different types of double-layer porous road pavement are investigated. The first type has a coarse porous surface and the second type has a fine porous surface. Both types of double-layer porous road pavement are currently used in the Netherlands[18] and are selected for the current study. Figures 13 and 14 illustrate the comparison of a double layer of porous road pavement with that of a single layer of road pavement. The spectra of sound amplification above a hard ground are also given in the figures for the purpose of comparison.

In Fig. 13, the acoustical structural parameters of the coarse top layer are given by $R_s = 6000\ \mathrm{N\,s\,m^{-4}}$, $\Omega = 20\%$, $q^2 = 3.5$, and $l_1 = 0.025$ m. For the bottom layer, $R_s = 1500\ \mathrm{N\,s\,m^{-4}}$, $\Omega = 20\%$, $q^2 = 4$, and $l_2 = 0.045$ m are used in Fig. 13. On the other hand, the predicted amplification factors for the porous road pavement with a fine top layer are shown in Fig. 14. The respective acoustical structural parameters of the top and bottom layers are given as follows. For the top layer, $R_s = 24\,000\ \mathrm{N\,s\,m^{-4}}$, $\Omega = 20\%$, $q^2 = 2.5$, and $l_1 = 0.015$ m, and, for the bottom layer, $R_s = 1500\ \mathrm{N\,s\,m^{-4}}$, $\Omega = 25\%$, $q^2 = 4$, and $l_1 = 0.055$ m.

It is not surprising to see that a double layer of porous road pavement can provide better attenuation of the horn amplification by creating more interference dips in the frequency range of interest. The first dip shifts to the lower frequency region in the case of a double layer of porous road pavement.

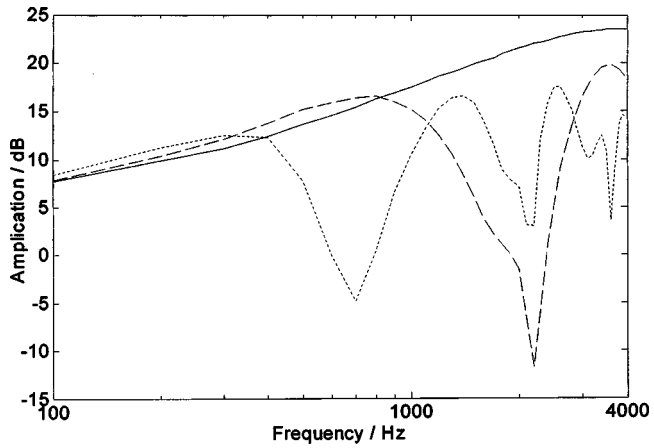

FIG. 13. Reduction in the horn effect due to a double layer of porous road pavement—the top layer is a coarse porous surface. (Solid line: hard ground; dashed line: a coarse top layer with $R_s = 6000\ \mathrm{N\,s\,m^{-4}}$, $\Omega = 20\%$, $q^2 = 3.5$, and $l_1 = 0.025$ m; dotted line: double layers—a coarse top layer and a bottom layer with $R_s = 1500\ \mathrm{N\,s\,m^{-4}}$, $\Omega = 25\%$, $q^2 = 4$, and $l_2 = 0.045$ m.)

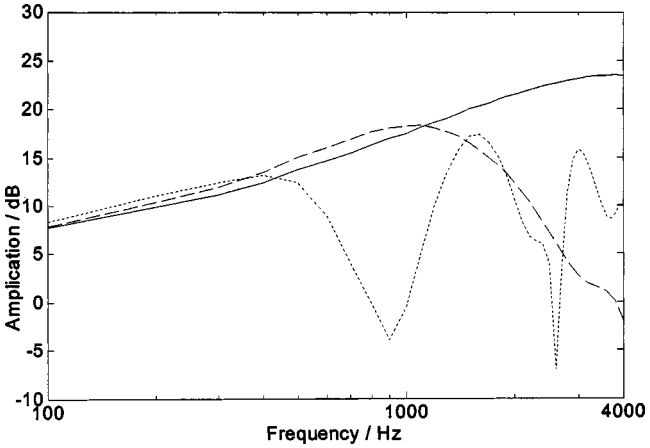

FIG. 14. Reduction in the horn effect due to a double layer of porous road pavement—the top layer is a fine porous surface. (Solid line: hard ground; dashed line: a fine top layer with $R_s = 24\,000$ N s m^{-4}, $\Omega = 20\%$, $q^2 = 2.5$ and $l_1 = 0.015$ m; dotted line: double layers—a fine top layer and a bottom layer with $R_s = 1500$ N s m^{-4}, $\Omega = 25\%$, $q^2 = 4$, and $l_2 = 0.055$ m.)

The dependence of the horn effect on the angular position of the source on the surface of the sphere is presented in Fig. 15. It shows that the amplification factor is rather insensitive to changes in the angular position of the source. There is a slight tendency for the interference dips to shift to lower frequencies when the angular position of the source increases.

Finally, a general remark can be drawn by studying Figs. 10–15: the acoustical properties of a porous layer and the angular position of the source on the surface of a tire do not have a noticeable influence on the horn effect at the low frequency region below 300 Hz.

V. CONCLUSIONS

This paper has contributed a theoretical model to study the amplification of noise due to the propagation of sound confined to a gap between the tire and the road over a porous road pavement. The simplified model can give good predictions of the general trend of amplification spectra compared to the published numerical and experimental results for the studies of the horn effect above hard and porous types of ground. The principal aim of this simplified model is to provide a parametric study of the acoustical parameters of porous road pavements on the horn effect. In the study, the source of the noise is assumed to be a monopole point source localized on the surface of the tire. It has been shown that a porous road pavement can effectively reduce the level of sound amplification resulting from the horn geometry of the tire/road in the frequency range of interest. A decrease in the thickness of the porous layer leads to an increase in the sound amplification of the horn effect. An increase in porosity or the use of a double layer of porous road pavement can enhance the attenuation of sound and create more interference dips in the amplification spectrum. The interference dips shift to lower frequencies when porosity increases or when a double layer of porous road pavement is used. However, changes in the flow resistivity of a porous road pavement do not seem to have a significant effect on horn amplification. As shown in the predictions, the variations in the angular position of the source on the tire surface have no significant effect on the horn amplification of sound.

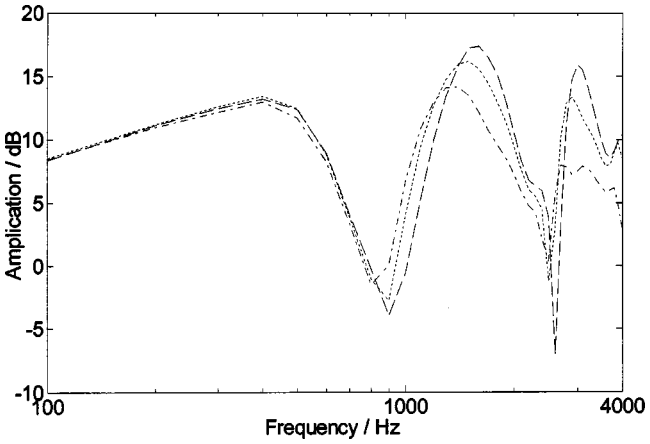

FIG. 15. Dependence of the horn effect on the angular position of the source on the surface of the tire. A fine double layer of porous road pavement is used for the simulation. (Dashed line: source at $\psi = 5°$; dotted line: source at $\psi = 10°$; dash-dotted line: source at $\psi = 15°$.)

ACKNOWLEDGMENTS

The research described in this paper was financed jointly by the Innovation and Technology Commission of the Hong Kong Special Administrative Region and the Mass Transit Railway Corporation Limited, through the award of a grant from the Innovation and Technology Fund under the category of the University-Industry Collaboration Program (Project No. UIM/39). The project was supported in part by the Research Grants Council of the Hong Kong Special Administrative Region (Project No. 8-Q334). The authors gratefully acknowledge the technical and administrative support given by the Hong Kong Polytechnic University.

[1] K. Iwao and I. Yamazaki, "A study on the mechanism of tire/road noise," JSAE Rev. **17**, 139–144 (1996).
[2] J. Perisse, "A study of radial vibrations of a rolling tire for tire-road noise characterization," Mech. Syst. Signal Process. **16**, 1043–1058 (2002).
[3] K. Larsson, S. Barrelet, and W. Kropp, "The modeling of the dynamic behaviour of tire tread blocks," Appl. Acoust. **63**, 659–677 (2002).
[4] M. Heckl, "Tire noise generation," Wear **13**, 157–170 (1986).
[5] K. Schaaf and D. Ronneberger, "Noise radiation from rolling tires—sound amplification by the horn effect," *Inter-Noise* **82**, San Francisco, CA, pp. 131–134.
[6] W. Kropp, F.-X. Becot, and S. Barrelet, "On the sound radiation from tyres," Acta Acust. **86**, 769–779 (2000).
[7] M. Ochmann, "The source simulation technique for acoustic radiation problems," Acustica **81**, 512–526 (1995).
[8] R. A. G. Graf, C.-Y. Kuo, A. P. Dowling, and W. R. Graham, "On the horn effect of a tire/road interface, Part I: experiment and computation," J. Sound Vib. **256**, 417–431 (2002).
[9] A. Fadavi, D. Duhamel, P. Klein, and F. Anfosso-Ledee, "Tire/road noise: 3D model for horn effect," Inter-noise 2000, Nice, France, 2000.
[10] F. Anfosso-Ledee, P. Klein, A. Fadavi, and D. Duhamel, "Tire/road noise: comparison of 2D and 3D models for horn effect," *Inter-Noise 2000*, Nice, France, 2000.
[11] C.-Y. Kuo, R. A. G. Graf, A. P. Dowling, and W. R. Graham, "On the horn effect of a tire/road interface, Part II: asymptotic theories," J. Sound Vib. **256**, 433–445 (2002).
[12] K. Attenborough, "Review of ground effects on outdoor sound propagation from continuous broadband sources," Appl. Acoust. **24**, 289–319 (1988).
[13] T. F. W. Embleton, "Tutorial on sound propagation outdoors," J. Acoust. Soc. Am. **100**, 31–48 (1996).

[14] K. M. Li, T. W. Fuller, and K. Attenborough, ''Sound propagation from a point source over extended-reaction ground,'' J. Acoust. Soc. Am. **104**, 679–685 (1998).
[15] S. Iwai, Y. Miura, H. Koike, and G. Levy, ''Influence of porous asphalt pavement characteristics on the horn amplification of tire/road contact noise,'' *Inter-Noise 94*, Yokohama, Japan, 1994.
[16] M. C. Bérengier, M. R. Stinson, G. A. Daigle, and J. F. Hamet, ''Porous road pavements: Acoustical characterization and propagation effects,'' J. Acoust. Soc. Am. **101**, 155–162 (1997).
[17] T. Iwase, ''Measurements of basic acoustical properties of the porous pavement and their applications to the estimation of road traffic noise reduction,'' J. Acoust. Soc. Jpn. **20**(1), 63–74 (1999).
[18] A. Kuijpers and G. Van Blokland, ''Modeling and optimization of two-layer porous asphalt roads,'' *Inter-Noise 2000*, Nice, France, 2000.
[19] T. Iwase, ''Acoustic properties of porous pavement with double layers and its reduction effects for road traffic noise,'' *Inter-Noise 2000*, Nice, France, 2000.
[20] K. M. Li, W. K. Lui, and G. H. Frommer, ''The diffraction of sound by an impedance sphere in the vicinity of a ground surface,'' J. Acoust. Soc. Am. **115**, 42–56 (2004).
[21] K. M. Li, W. K. Lui, and G. H. Frommer, ''The scattering of sound by a hard sphere above an impedance ground,'' Acta Acust. **90**, 251–262 (2004)